

Power Maximization for a Multiport Network Described by the Admittance Matrix

Ben Minnaert, Giuseppina Monti, Alessandra Costanzo, and Mauro Mongiardo

Abstract – This work analyzes a general (reciprocal or nonreciprocal) multiport system described by its admittance matrix. The general case of a link using a multiple-input and multiple-output configuration is solved by determining the optimal loads for maximizing the total power delivered to the loads. As a specific application of interest, the proposed theory is demonstrated on a wireless link based on capacitive coupling.

1. Introduction

Consider a multiport network with an arbitrary number of input and output ports. The input ports are fed by power supplies. The purpose of this paper is to propose an easy procedure to determine the terminations of the multiport network that maximize the power transfer to the output ports.

The multiport network is considered as a black box and can be any physical network. In this work, focus is on multiport networks for which it is convenient to fully characterize the multiport by its admittance matrix \mathbf{Y} . Application examples include the following:

- Coupled transmission lines, e.g., multiconductor transmission lines in power systems for efficient transmission of electrical energy from one point to another [1, 2].
- Any form of wireless power transfer (WPT) systems such as microwave/RF WPT or near-field WPT. In particular *capacitive* WPT can be easier described by its admittance matrix [3], contrary to an *inductive* WPT multiport, which is more manageable if characterized by its impedance matrix [4].
- Propagation channels of multiple-input multiple-output (MIMO) networks [5].
- Microwave filters and couplers [6, 7].
- Nonreciprocal circuit networks such as ferrite isolators [7].

Manuscript received 26 August 2020.

Ben Minnaert is with the Odisee University College of Applied Sciences, Ghent, Belgium; ben.minnaert@odisee.be.

Giuseppina Monti is with the Department of Engineering for Innovation, University of Salento, Lecce, Italy; giuseppina.monti@unisalento.it.

Alessandra Costanzo is with the Department of Electrical, Electronic and Information Engineering “Guglielmo Marconi,” University of Bologna, Bologna, Italy; alessandra.costanzo@unibo.it.

Mauro Mongiardo is with the Department of Engineering, University of Perugia, Perugia, Italy; mauro.mongiardo@unipg.it.

This work is an extension on [8] that described the method for a reciprocal wireless power transfer system. In the current work, we emphasize that the method is applicable to *any reciprocal or nonreciprocal* multiport network. Compared to [8], it now includes the calculation of the maximum output power, corresponding input power, and system efficiency (power gain) of the network. Moreover, the numerical verification is more elaborated by explicitly adding the admittance matrix and the simulation circuit in SPICE of a capacitive multiport example.

2. Multiport Representation With M Input and N Output Ports

A multiport network N' with M input and N output ports is considered and fully characterized by its admittance matrix \mathbf{Y} . The M input ports of the network are connected to M current sources (Figure 1, left side). At the N output ports, loads admittances $Y_{L,i} = G_{L,i} + j \cdot B_{L,i}$ are present ($i = 1, \dots, N$), with $G_{L,i}$ and $B_{L,i}$ the load conductance and load susceptance, respectively (Figure 1, right side). The peak current and voltage phasors at the M input and N output ports, respectively, are defined in Figure 1. The following matrices are introduced:

$$\mathbf{i}_M = \begin{bmatrix} I_1 \\ I_2 \\ I_3 \\ \vdots \\ I_M \end{bmatrix}, \mathbf{v}_M = \begin{bmatrix} V_1 \\ V_2 \\ V_3 \\ \vdots \\ V_M \end{bmatrix}, \mathbf{i}_N = \begin{bmatrix} I_{L,1} \\ I_{L,2} \\ I_{L,3} \\ \vdots \\ I_{L,N} \end{bmatrix}, \mathbf{v}_N = \begin{bmatrix} V_{L,1} \\ V_{L,2} \\ V_{L,3} \\ \vdots \\ V_{L,N} \end{bmatrix} \quad (1)$$

The relation between the voltages and the currents of the multiport can be described by

$$\begin{bmatrix} \mathbf{i}_M \\ \mathbf{i}_N \end{bmatrix} = \begin{bmatrix} \mathbf{Y}_{MM} & \mathbf{Y}_{MN} \\ \mathbf{Y}_{NM} & \mathbf{Y}_{NN} \end{bmatrix} \cdot \begin{bmatrix} \mathbf{v}_M \\ \mathbf{v}_N \end{bmatrix} \quad (2)$$

where the admittance matrix of the network N' has been partitioned into four submatrices \mathbf{Y}_{MM} , \mathbf{Y}_{MN} , \mathbf{Y}_{NM} , and \mathbf{Y}_{NN} . The subscripts of the submatrices indicate their dimension.

By applying the Norton's theorem, for the multiport network it is possible to derive the equivalent circuit illustrated in Figure 2, where the currents $I_i^{(no)}$ are the Norton currents ($i = 1, \dots, N$). Notice that the M input ports are replaced by open circuits. The N loads of the receiver are represented by the network N_L , described by the admittance matrix \mathbf{Y}_L .

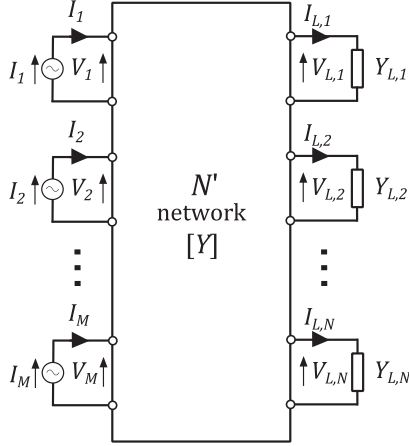


Figure 1. At a multiport network N' , characterized by its admittance matrix \mathbf{Y} , are M current sources (left side) and N loads (right side) connected.

The Norton currents can be derived by short-circuiting the output ports ($\mathbf{v}_N = \mathbf{0}$) and equal the following [8]:

$$\mathbf{i}_N = \mathbf{Y}_{NM} \mathbf{Y}_{MM}^{-1} \cdot \mathbf{i}_M \equiv \mathbf{i}_N^{(\text{no})} = \begin{bmatrix} I_1^{(\text{no})} \\ I_2^{(\text{no})} \\ I_3^{(\text{no})} \\ \vdots \\ I_N^{(\text{no})} \end{bmatrix} \quad (3)$$

The Norton admittance matrix \mathbf{Y}_0 , which characterizes network N_0 , is defined by

$$\mathbf{i}_N = \mathbf{Y}_0 \cdot \mathbf{v}_N \quad (4)$$

It can be expressed as function of the elements of the original admittance matrix \mathbf{Y} of the multiport [8]:

$$\mathbf{Y}_0 = \mathbf{Y}_{NN} - \mathbf{Y}_{NM} \cdot \mathbf{Y}_{MM}^{-1} \cdot \mathbf{Y}_{MN} \quad (5)$$

3. Optimal Loads for Power Maximization

The goal of this work is to determine the loads that realize maximum power transfer from the M input ports to the N output ports, i.e., that maximize the total output power P_{out} defined as

$$P_{\text{out}} = \sum_{i=1}^N P_i \quad (6)$$

with P_i the output power delivered to load $Y_{L,i}$. By applying Norton's theorem, the original circuit of Figure 1 was replaced by the equivalent circuit of Figure 2 with Norton admittance matrix \mathbf{Y}_0 and current sources $I_i^{(\text{no})}$.

Spinei [9] determined a generalized condition for the voltage-current relations at the ports of a multiport network for achieving maximum power transfer to passive loads:

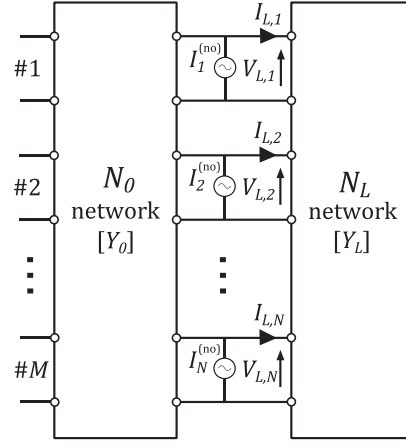


Figure 2. Norton equivalent circuit with load network N_L .

$$\mathbf{v}_N = (\mathbf{Y}_0 + \mathbf{Y}_0^+)^{-1} \mathbf{i}^{(\text{no})} \quad (7)$$

with \mathbf{Y}_0^+ the conjugate transpose of \mathbf{Y}_0 . For a reciprocal network the conjugate transpose coincides with the conjugate. The procedure described in this work is also valid for nonreciprocal networks.

Since \mathbf{Y}_0 and $\mathbf{i}^{(\text{no})}$ are known from the previous section, the optimal voltages \mathbf{v}_N at the N output ports that realize maximum power transfer are known.

Substituting (7) into the network equations of Figure 2 results in the optimal currents [8]:

$$\mathbf{i}_N = \mathbf{i}^{(\text{no})} - \mathbf{Y}_0 (\mathbf{Y}_0 + \mathbf{Y}_0^+)^{-1} \mathbf{i}^{(\text{no})} \quad (8)$$

Equations (7) and (8) determine the voltages and currents at the loads for the maximum power configuration. The load admittances that realize maximum power transfer are therefore given by

$$Y_{L,i} = G_{L,i} + jB_{L,i} = \frac{I_{L,i}}{V_{L,i}} \quad (9)$$

where $i = 1, \dots, N$, with $V_{L,i}$ and $I_{L,i}$ the elements of \mathbf{v}_N and \mathbf{i}_N , respectively, as described by (7) and (8).

The procedure to find the loads for power maximization for a multiport network can be summarized as follows:

- 1) Establish (e.g., by measurement or simulation) the admittance matrices \mathbf{Y}_{MM} , \mathbf{Y}_{MN} , \mathbf{Y}_{NM} , and \mathbf{Y}_{NN} of the multiport network given by (2).
- 2) Determine the Norton current sources $\mathbf{i}_N^{(\text{no})}$ from (3).
- 3) Set up the Norton admittance matrix \mathbf{Y}_0 using (5).
- 4) Calculate the voltages \mathbf{v}_N (see (7)) and currents \mathbf{i}_N (see (8)) for the loads at the maximum power configuration.
- 5) Determine the optimal loads $Y_{L,i}$ from (9).

This procedure maximizes the power output P_{out} as defined in (6). Its value can be calculated by

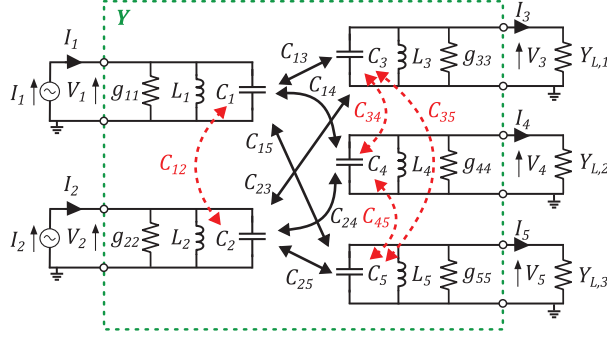


Figure 3. Equivalent circuit of a capacitive WPT system with two transmitters and three receivers.

$$P_{\text{out}} = \frac{1}{4}(\mathbf{v}_N^+ \cdot \mathbf{i}_N + \mathbf{i}_N^+ \cdot \mathbf{v}_N) \quad (10)$$

Also the input power P_{in} (i.e., the sum of the input powers at each of the M input ports) can now easily be calculated:

$$P_{\text{in}} = \frac{1}{4}(\mathbf{v}_M^+ \cdot \mathbf{i}_M + \mathbf{i}_M^+ \cdot \mathbf{v}_M) \quad (11)$$

and thus also the system efficiency or power gain η :

$$\eta = \frac{P_{\text{out}}}{P_{\text{in}}} \quad (12)$$

4. Numerical Verification

The theory presented in the previous section is valid for any multiport network, regardless of the total number of $(M + N)$ ports and its specific implementation; in order to be applied, the presented methodology just requires the experimental or analytical derivation of the admittance matrix of the network. In this section, the procedure is demonstrated and numerically verified on an example application: a capacitive WPT system with two transmitters ($M = 2$) and three receivers ($N = 3$). The approximated equivalent circuit of the analyzed link is illustrated in Figure 3 [10].

At the two input ports (Figure 3, left side), two current sources I_1 and I_2 power the system. At the three output ports (Figure 3, right side), load admittances $Y_{L,1}$, $Y_{L,2}$, and $Y_{L,3}$ are connected. The voltages V_j and currents I_j at the ports are defined in the figure ($j = 1, \dots, 5$).

The shunt conductances g_{ij} describe the losses in the circuit. The mutual capacitances $C_{13}, C_{14}, C_{15}, C_{23},$

Table 1. Given circuit parameters of the example capacitive WPT system

Quantity	Value	Quantity	Value
g_{11}	1.00 mS	C_1	350 pF
g_{22}	1.25 mS	C_2	300 pF
g_{33}	1.50 mS	C_3	250 pF
g_{44}	1.75 mS	C_4	225 pF
g_{55}	2.00 mS	C_5	200 pF
I_1	100 mA	f_0	10 MHz
I_2	200 mA		

Table 2. Coupling factors of the analyzed numerical example

Desired coupling	Value (%)	Undesired coupling	Value (%)
k_{13}	30	k_{12}	10
k_{14}	25	k_{34}	5
k_{15}	20	k_{35}	2
k_{23}	25	k_{45}	5
k_{24}	20		
k_{25}	15		

C_{24} , and C_{25} represent the desired electric coupling between the transmitter capacitances C_1, C_2 , and the receiver capacitances C_3, C_4, C_5 . They realize the wireless link between transmitters and receivers [6]. Undesired electric coupling is present between both transmitters, indicated by the mutual capacitance C_{12} . An undesired coupling also is present between the receivers: C_{34}, C_{35} , and C_{45} .

To obtain a resonant scheme, the inductors $L_j = 1/\omega_0^2 C_j$ are added with ω_0 the operating angular frequency of the current sources I_1 and I_2 . The coupling factor k_{ij} is defined as $k_{ij} = C_{ij}/\sqrt{C_i C_j}$ ($i, j = 1, \dots, 5$).

As an example, consider the system with numerical values indicated in Table 1 and operating at $f_0 = 10$ MHz. The entire multiport system (indicated by the dashed rectangle in Figure 3) is fully determined by the admittance matrix \mathbf{Y} , which is, at the resonance angular frequency ω_0 , equal to

$$\mathbf{Y} = \begin{bmatrix} \mathbf{Y}_{MM} & \mathbf{Y}_{MN} \\ \mathbf{Y}_{NM} & \mathbf{Y}_{NN} \end{bmatrix} = \begin{bmatrix} 1.00 & -2.04j & -5.58j & -4.41j & -3.32j \\ -2.04j & 1.25 & -4.30j & -3.26j & -2.31j \\ -5.58j & -4.30j & 1.50 & -0.745j & -0.281j \\ -4.41j & -3.26j & -0.745j & 1.75 & -0.666j \\ -3.32j & -2.31j & -0.281j & -0.666j & 2.0 \end{bmatrix} \text{ mS} \quad (13)$$

with nondiagonal elements $\omega_0 C_{ij}$. The coupling factors between the transmitters and receivers are indicated in Table 2.

By using (9), the values reported in Table 3 can be obtained for the optimal terminating admittances. The optimal load susceptances are negative, i.e., they correspond to shunt inductors whose values are reported in the table.

To verify the analytical results summarized in Table 3 circuitual simulations have been performed in SPICE. The equivalent pi circuit for coupled capacitors, valid near resonance, is applied (Figure 4). The simulations are executed in the time domain with maximum time step 1 ps. First, a simulation with the network terminated on the optimal admittances given in

Table 3. Optimal terminating admittances for the analyzed numerical example

$G_{L,1}$ (mS)	$L_{L,1}$ (μH)	$G_{L,2}$ (mS)	$L_{L,2}$ (μH)	$G_{L,3}$ (mS)	$L_{L,3}$ (μH)
21.4	524.0	23.0	443.0	22.6	370.0

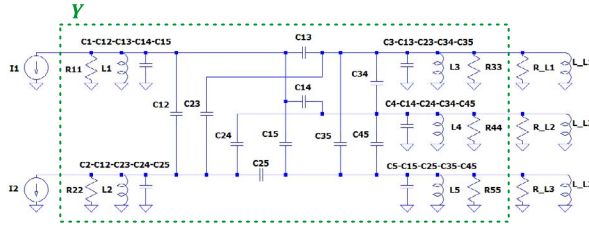


Figure 4. The circuit in SPICE simulating a system with two transmitters and three receivers. The resistances R_{ii} are applied for the corresponding conductances g_{ii} ($i = 1, \dots, N$). The coupled capacitors are represented by the equivalent pi circuits. R_{Ln} and L_{Ln} ($n = 1, 2, 3$) depict the load resistances and load susceptances.

Table 3 has been performed; SPICE returns an output power of 4.64 W, which corresponds to the value calculated by (10). Next, six simulations were performed by varying among the six parameters of interest one parameter at a time (either one of the three conductances G_{Li} or one of the load inductors $L_{L,i}$) while keeping all the others constant at their optimal value shown in the Table 3.

The achieved results are reported in Figures 5 and 6. They confirm the data provided by the theory for this example: a maximum power output is achieved when the loads are the ones calculated according to (9).

Note that maximizing the power output does not maximize the system efficiency η (or power gain). SPICE returns an efficiency of 48.7%, which corresponds to the value calculated by (12). Moreover, the maximum power output configuration also does not realize a uniform power distribution. The relative output power delivered to the first, second, and third load is 59%, 29%, and only 12%, respectively.

5. Conclusions

A procedure to easily find the optimal load values to maximize the power transfer for a

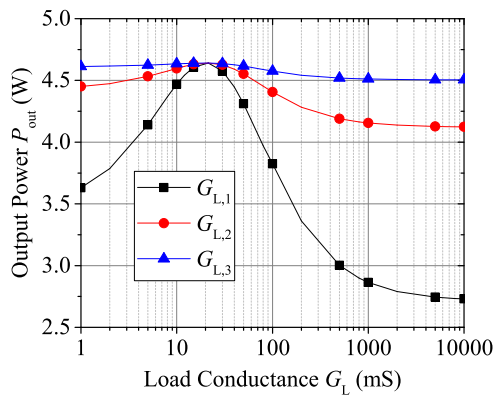


Figure 5. Simulated output power P_{out} as function of varying load conductance for the analyzed numerical example. One of the three load conductances is varied while keeping the other two fixed at their optimal value.

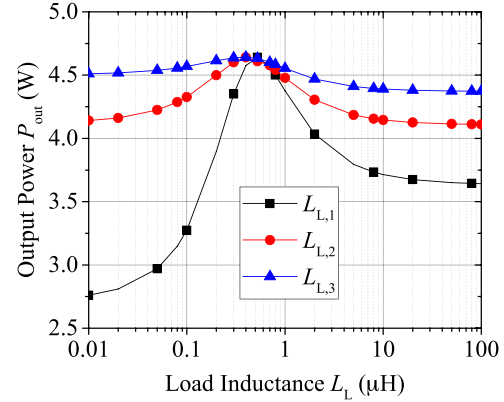


Figure 6. Simulated output power P_{out} as function of varying load inductance for the analyzed numerical example. One of the three load inductances is varied while keeping the other two fixed at their optimal value.

(reciprocal or nonreciprocal) multiport network has been presented. The proposed methodology is valid for *any* number of input and output ports. The calculation of the optimal loads requires just the knowledge of the admittance matrix of the system, which can be analytically calculated or measured. The reported formulas are validated through circuitual simulations performed for a numerical example referring to a capacitive link using three transmitters and two loads.

6. References

1. G. I. Zysman and A. K. Johnson, "Coupled Transmission Line Networks in an Inhomogeneous Dielectric Medium," *IEEE Transactions on Microwave Theory and Techniques*, **17**, 10, 1969, pp. 753-759.
2. V. K. Tripathi and H. Lee, "Spectral-Domain Computation of Characteristic Impedances and Multiport Parameters of Multiple Coupled Microstrip Lines," *IEEE Transactions on Microwave Theory and Techniques*, **37**, 1, 1989, pp. 215-221.
3. B. Minnaert and N. Stevens, "Optimal Analytical Solution for a Capacitive Wireless Power Transfer System With One Transmitter and Two Receivers," *Energies*, **10**, 9, 2017, p. 1444.
4. G. Monti, Q. Wang, W. Che, A. Costanzo, F. Matri, and M. Mongiardo, "Maximum Wireless Power Transfer for Multiple Transmitters and Receivers," in *Proceedings of IEEE MTT-S NEMO*, 2016, pp. 1-3.
5. X. Yu, L. Wang, H. G. Wang, X. Wu, and Y. H. Shang, "A Novel Multiport Matching Method for Maximum Capacity of an Indoor MIMO System," *Progress in Electromagnetics Research*, **130**, 2012, pp. 67-84.
6. J. S. G. Hong and M. J. Lancaster, *Microstrip Filters for RF/Microwave Applications*, New York, John Wiley & Sons, 2001.
7. D. M. Pozar, *Microwave Engineering, 4th Edition*, New York, John Wiley & Sons, 2012.
8. B. Minnaert, G. Monti, F. Matri, A. Costanzo, and M. Mongiardo, "Power Maximization for a Multiple-Input and Multiple-Output Wireless Power Transfer System Described by the Admittance Matrix," presented in the

XXXIV General Assembly and Scientific Symposium of the International Union of Radio Science, URSI GASS 2020, 29 August to 5 September 2020.

9. F. Spinei, "On Generalizations of the Maximum Power

Transfer Problem," *Proceedings of the IEEE*, **60**, 7, 1972, pp. 903-904.

10. J. Kracek and M. Svanda, "Analysis of Capacitive Wireless Power Transfer," *IEEE Access*, **7**, 2018, pp. 26678-26683.